2

Electrode Size and Dimensional Ratio Effect on the Resonant Characteristics of Piezoelectric Ceramic Disk

Lang Wu[1], Ming-Cheng Chure[1], Yeong-Chin Chen[2], King-Kung Wu[1] and Bing-Huei Chen[3]
[1]*Department of Electronics Engineering, Far-East University,*
[2]*Department of Computer Science & Information Engineering, Asia University,*
[3]*Department of Electrical Engineering, Nan Jeon Institute of Technology, Taiwan*

1. Introduction

After discovered at 1950, lead zirconate titanate [$Pb(Zr,Ti)O_3$; PZT] ceramics have intensively been studied because of their excellent piezoelectric properties [Jaffe et al., 1971; Randeraat & Setterington, 1974; Moulson & Herbert, 1997; Newnham & Ruschau, 1991; Hertling, 1999]. The PZT piezoelectric ceramics are widely used as resonator, frequency control devices, filters, transducer, sensor and etc. In practical applications, the piezoelectric ceramics are usually circular, so the vibration characteristics of piezoelectric ceramic disks are important in devices design and application. The vibration characteristics of piezoelectric ceramics disk had been study intensively by many of the researchers [Shaw, 1956; Guo et al., 1992; Ivina, 1990a, 2001b; Kunkel et al., 1990; Masaki et al., 2008]. Shaw [Shaw, 1956] measured vibrational modes in thick barium titanate disks having diameter-to-thickness ratios between 1.0 and 6.6**.** He used an optical interference technique to map the surface displacement at each resonance frequency, and used a measurement of the resonance and antiresonance frequency to calculate an electromechanical coupling for each mode. Guo et al., [Guo et al., 1992] presented the results for PZT-5A piezoelectric disks with diameter-to-thickness ratios of 20 and 10. There were five types of modes being classified according to the mode shape characteristics, and the physical interpretation was well clarified. Ivina [Ivina, 1990] studied the symmetric modes of vibration for circular piezoelectric plates to determine the resonant and anti-resonant frequencies, radial mode configurations, and the optimum geometrical dimensions to maximize the dynamic electromechanical coupling coefficient. Kunkel et al., [Kunkel et al., 1990] studied the vibration modes of PZT-5H ceramics disks concerning the diameter-to-thickness ratio ranging from 0.2 to 10. Both the resonant frequencies and effective electromechanical coupling coefficients were calculated for the optimal transducer design. Masaki et al., [Masaki et al., 2008] used an iterative automated procedure for determining the complex materials constants from conductance and susceptance spectra of a ceramic disk in the radial vibration mode.

The phenomenon of partial-electroded piezoelectric ceramic disks also study by some researchers. Ivina [Ivina, 2001] analyzed the thickness symmetric vibrations of piezoelectric disks with partial axisymmetric electrodes by using the finite element method. According to the spectrum and value of the dynamic electromechanical coupling coefficient of quasi-thickness vibrations, the piezoelectric ceramics can be divided into two groups. Only for the first group can the DCC be increased by means of the partial electrodes, which depends on the vibration modes. Schmidt [Schmidt, 1972] employed the linear piezoelectric equations to investigate the extensional vibrations of a thin, partly electroded piezoelectric plate. The theoretical calculations were applied to the circular piezoelectric ceramic plate with partial concentric electrodes for the fundamental resonant frequency. Huang [Huang, 2005] using the linear two-dimensional electroelastic theory, the vibration characteristics of partially electrode-covered thin piezoelectric ceramic disks with traction-free boundary conditions are investigated by theoretical analysis, numerical calculation, and experimental measurement.

In this study, the vibration characteristics of a thin piezoelectric ceramic disk with different electrode size and dimensional ratio are study by the impedance analysis method.

2. Vibration analysis of the piezoelectric ceramic disk

Figure 1 shows the geometrical configuration of the piezoelectric ceramic disk with radius R and thickness h. The piezoelectric ceramic disk is assumed to be thin (R>>h) and polarized in the thickness direction. If the cylindrical coordinates (r, θ, z) with the origin in the center of the disk are used. The linear piezoelectric constitutive equations of a piezoelectric ceramic with crystal symmetry C_{6mm}, can be expressed as [IEEE, 1987]:

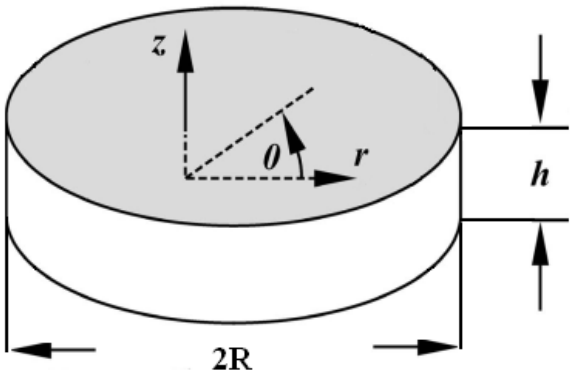

Fig. 1. The geometrical configuration of the piezoelectric ceramic disk.

$$\begin{bmatrix} S_{rr} \\ S_{\theta\theta} \\ S_{zz} \\ S_{\theta z} \\ S_{rz} \\ S_{r\theta} \\ D_r \\ D_\theta \\ D_z \end{bmatrix} = \begin{bmatrix} s_{11}^E & s_{12}^E & s_{13}^E & 0 & 0 & 0 & 0 & 0 & d_{31} \\ s_{12}^E & s_{11}^E & s_{13}^E & 0 & 0 & 0 & 0 & 0 & d_{31} \\ s_{13}^E & s_{13}^E & s_{33}^E & 0 & 0 & 0 & 0 & 0 & d_{33} \\ 0 & 0 & 0 & s_{44}^E & 0 & 0 & 0 & d_{15} & 0 \\ 0 & 0 & 0 & 0 & s_{44}^E & 0 & d_{15} & 0 & 0 \\ 0 & 0 & 0 & 0 & 0 & s_{66}^E & 0 & 0 & 0 \\ 0 & 0 & 0 & 0 & d_{15} & 0 & \varepsilon_{11}^T & 0 & 0 \\ 0 & 0 & 0 & d_{15} & 0 & 0 & 0 & \varepsilon_{11}^T & 0 \\ d_{31} & d_{31} & d_{33} & 0 & 0 & 0 & 0 & 0 & \varepsilon_{33}^E \end{bmatrix} \begin{bmatrix} T_{rr} \\ T_{\theta\theta} \\ T_{zz} \\ T_{\theta z} \\ T_{rz} \\ T_{r\theta} \\ E_r \\ E_\theta \\ E_z \end{bmatrix} \tag{1}$$

where T_{rr}, $T_{\theta\theta}$ and T_{zz} are the longitudinal stress components in the r, θ and z directions; $T_{r\theta}$, $T_{\theta z}$ and T_{rz} are the shear stress components. S_{rr}, $S_{\theta\theta}$, S_{zz}, $S_{\theta z}$, S_{rz} and $S_{r\theta}$ are the strain components. D_r, D_θ and D_z are the electrical displacement components, and E_r, E_θ, and E_z are the electrical fields. $s_{11}^E, s_{12}^E, s_{13}^E, s_{33}^E, s_{44}^E$ and s_{66}^E are the compliance constants at constant electrical field, in which $s_{66}^E = 2(s_{11}^E - s_{12}^E)$. d_{15}, d_{31} and d_{33} are the piezoelectric constants; ε_{11}^T and ε_{33}^T are the dielectric constants.

The electric field vector E_i is derivable from a scalar electric potential V_j:

$$E_r = -\frac{\partial V}{\partial r} \tag{2a}$$

$$E_\theta = -\frac{1}{r}\frac{\partial V}{\partial \theta} \tag{2b}$$

$$E_z = -\frac{\partial V}{\partial z} \tag{2c}$$

The electric displacement vector D_i satisfies the electrostatic equation for an insulator, and shown as:

$$\frac{\partial D_r}{\partial r} + \frac{1}{r}\frac{\partial D_\theta}{\partial \theta} + \frac{1}{r}D_r + \frac{\partial D_z}{\partial z} = 0 \tag{3}$$

Some basic hypotheses are employed for analysis the vibration of thin disk [Rogacheva, N.N., 1994]:

a. Normal stress T_{zz} is very small, so it can be neglected relative to other stresses, hence $T_{zz} = 0$.
b. The rectilinear element normal to the middle surface before deformation remains perpendicular to the strained surface after deformation, and its elongation can be neglected, i.e., $S_{rz}=S_{\theta z} = 0$.
c. Electrical displacement D_z is a constant with respect to the thickness.

In this study, only the radial axisymmetry vibrations of the disk are considered, so S_{zz}=0. The electrodes are coated on the z axis, so E_r=0 and E_θ=0. The constitutive equations can reduce to:

$$S_{rr} = s_{11}^E T_{rr} + s_{12}^E T_{\theta\theta} + d_{31} E_z \tag{4a}$$

$$S_{\theta\theta} = s_{12}^E T_{rr} + s_{11}^E T_{\theta\theta} + d_{31} E_z \tag{4b}$$

$$S_{r\theta} = s_{66}^E T_{r\theta} = 2(s_{11}^E - s_{12}^E) T_{r\theta} \tag{4c}$$

$$D_z = d_{31} T_{rr} + d_{31} T_{\theta\theta} + \varepsilon_{33}^E E_z \tag{4d}$$

The stresses and the charge density Q on the surface of the disk, can be obtained by inversion of Eq.(4),

$$T_{rr} = \frac{1}{s_{11}^E (1-\sigma^2)} (S_{rr} + \sigma S_{\theta\theta}) - \frac{d_{31}}{s_{11}^E (1-\sigma)} \frac{2V_3}{h} \tag{5a}$$

$$T_{\theta\theta} = \frac{1}{s_{11}^E (1-\sigma^2)} (S_{\theta\theta} + \sigma S_{rr}) - \frac{d_{31}}{s_{11}^E (1-\sigma)} \frac{2V_3}{h} \tag{5b}$$

$$T_{r\theta} = \frac{1}{s_{66}^E} S_{r\theta} = \frac{S_{r\theta}}{2(s_{11}^E - s_{12}^E)} = \frac{S_{r\theta}}{2s_{11}^E (1+\sigma)} \tag{5c}$$

$$D_z = d_{31} (S_{rr} + S_{\theta\theta}) + \varepsilon_{33}^T \frac{2V_3}{h} \tag{5d}$$

where σ is Poisson's ratio and equal to $-(s_{11}^E / s_{12}^E)$, V_3 is the voltage applied in the z-direction.

Assumed the radial extensional displacement of the middle plane as:

$$u_r(r,t) = U(r) e^{i\omega t} \tag{6}$$

where ω is the angular frequency.

The strain-mechanical displacement relations are:

$$S_{rr} = \frac{\partial U}{\partial r} \tag{7a}$$

$$S_{\theta\theta} = \frac{U}{r} \tag{7b}$$

$$S_{r\theta} = \frac{1}{r} \frac{\partial U}{\partial \theta} \tag{7c}$$

Then the stress-displacement relations of the radial vibration are given as:

$$T_{rr} = \frac{1}{s_{11}^E(1-\sigma^2)}\left(\frac{dU}{dr} + \sigma\frac{U}{r}\right) + \frac{d_{31}}{s_{11}^E(1-\sigma)}\frac{2V_3}{h} \tag{8a}$$

$$T_{\theta\theta} = \frac{1}{s_{11}^E(1-\sigma^2)}\left(\frac{U}{r} + \sigma\frac{dU}{dr}\right) + \frac{d_{31}}{s_{11}^E(1-\sigma)}\frac{2V_3}{h} \tag{8b}$$

and the charge density is:

$$Q = -\frac{d_{31}}{s_{11}^E(1-\sigma)}\left(\frac{\partial U}{\partial r} + \frac{U}{r}\right) - \frac{2d_{31}^2}{s_{11}^E(1-\sigma)}\frac{2V_3}{h} + \varepsilon_{33}^T\frac{2V_3}{h} \tag{9}$$

The equation of motion in the radial direction is

$$\frac{\partial T_{rr}}{\partial r} - rT_{\theta\theta} + \frac{1}{r}T_{rr} = \rho\frac{\partial^2 u_r}{\partial t^2} \tag{10}$$

where ρ is the density.

Substitution of Eq.(8) into Eq.(10), find

$$\frac{d^2U}{dr^2} + \frac{1}{r}\frac{dU}{dr} - \frac{1}{r^2}U - \rho\omega^2 s_{11}^E(1-\sigma^2)U = 0 \tag{11}$$

the general solution of Eq.(11) is

$$U(r)=CJ_1(\beta r) \tag{12}$$

where J_1 is the Bessel function of the first kind and first order, C is a constant and

$$\beta^2 = \rho s_{11}^E(1-\sigma^2)\omega^2 \tag{13}$$

For the boundary condition at r = R, it has:

$$\int_{-h/2}^{h/2} T_{rr}dz = 0 \tag{14}$$

So, the constant C is found to be:

$$C = \frac{2Vd_{31}(1+\sigma)}{(1-\sigma)J_1(\beta R) - \beta R J_0(\beta R)}\frac{R}{h} \tag{15}$$

where J_0 is Bessel function of the first kind and zero order.

When the piezoelectric disk in radial vibration, the current can be developed as[Huang et al, 2004]:

$$I = \frac{\partial}{\partial t}\iint_S D_z ds = i\omega \int_0^{2\pi}\int_0^R \left\{ \frac{d_{31}(1+\sigma)}{s_{11}^E(1-\sigma^2)}\left[\frac{dU}{dr}+\frac{U}{r}\right] + \frac{2\varepsilon_{33}^T V}{h}(k_p^2-1)\right\} r dr d\theta$$
$$= i\omega \frac{2\pi R^2 V \varepsilon_{33}^T}{h} \frac{\left[1-\sigma+(1+\sigma^2)\dfrac{k_p^2}{1-k_p^2}\right] J_1(\beta R) - \beta R J_0(\beta R)}{(1-\sigma)J_1(\beta R) - \beta R J_0(\beta R)} \tag{16}$$

where S is the area of the electrode and

$$k_p = \sqrt{\frac{2d_{31}^2}{\varepsilon_{33}^T s_{11}^E (1-\sigma)}} \tag{17}$$

is the planar effective electromechanical coupling factor.

The frequencies corresponding to the current I approaches infinity is the resonant frequencies. The characteristic equation of resonant frequencies for radial vibrations is given by:

$$\eta J_0(\eta) = (1-\sigma) J_1(\eta) \tag{18}$$

where $\eta = \beta R$.

The antiresonant frequencies for which the current through the piezoelectric ceramic disk equal to zero are determined from the roots of the following equation:

$$\left[1-\sigma+(1+\sigma)\frac{k_p^2}{k_p^2-1}\right] J_1(\eta) = \eta J_0(\eta) \tag{19}$$

From Eqs(12), (18) and (19), under free boundary conditions, the resonant frequency of the piezoelectric ceramic disk with fully coated electrode can be expressed as:

$$f_r = \frac{\eta}{2\pi R}\sqrt{\frac{1}{\rho s_{11}^E (1-\sigma^2)}} \tag{20}$$

3. Experimental process

The piezoceramic disks used in this study were prepared by conventional powder processing technique, starting from high purity raw materials, TiO_2 (Merck, 99%), ZrO_2 (Aldrich, 99%) and PbO (Merck, 99%). The compositions of the ceramics were in the vicinity of the MPB of PZT in the tetragonal range, and doped with minor MnO_2 and Sb_2O_3.

After 2h ball milling with ZrO_2 balls, the mixed powders were calcined in air for 2h at 850°C. The calcined powders were then cold pressed into disk type pellets. The pellets were sintered at 1250°C for 2h with the double crucible arrangement, with $PbZrO_3$ atmosphere powder for PbO compensation.

Two groups of samples were used in this study, one group used for electrode size study, the other group used for dimensional ratio effect. The diameter and thickness of samples used

for electrode size study were 15mm and 0.9mm, respectively. The (diameter/thickness) ratio of the samples used for the dimensional ratio effect was from 7.25 to 20.16.

Crystal phase structure was examined by a Rigaku X-ray diffraction (XRD) with CuKα radiation (λ=1.5418Å), scanned from 20° to 80° and scanning speed was 4°/min. Microstructures were analyzed on a polished surface of the specimens by high resolution scanning electron microscopy (SEM). The relative density of piezoelectric ceramics was measured by an Archimedes's method.

The flat surfaces of the samples were polished, cleaned and coated with silver electrode to get a better Ohmic contact for electric properties measurement. There are total five different electrode size used for electrode size study, as list in Table-1. After electrode coating, the samples were poled under 3.0 kV/mm electric field at elevated temperature 100°C for 1h in the silicone oil bath. After polarization, the piezoelectric properties were surveyed with an HP4194A Impedance/Gain-Phase Analyzer and Berlincourt d_{33} meter based on the IEEE standards [IEEE, 1987]. Resonant spectrum of the samples was determined in the frequency range from 100 kHz to 1500 kHz, and the results were recorded by a PC base data acquisition system.

No.	D1	D2	D3	D4	D5
Electrode Size	100%	80%	60%	40%	20%

Table 1. Electrode size used in this study.

4. Results and discussions

Figure 2 shows the SEM micrographs of the sintered ceramics body, and the grain size of the ceramics body was less than 2μm. The XRD pattern of the ceramics before poling was shown in Fig.3. The crystal structure of the ceramics is tetragonal perovskite, with a=4.036Å, c=4.102Å and tetragonality c/a=1.016.

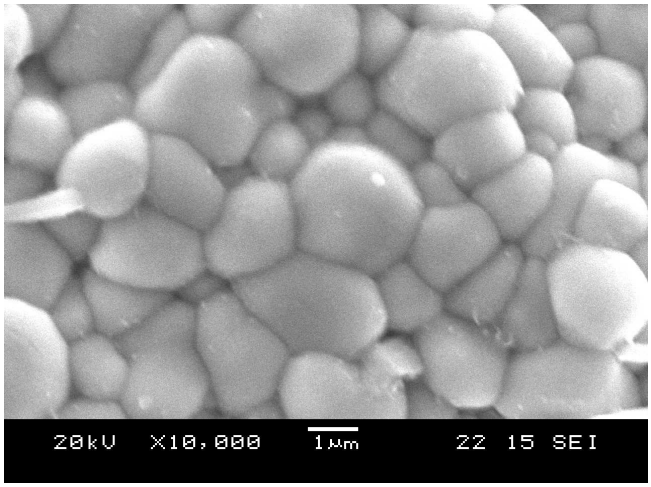

Fig. 2. SEM micrographs of the sintered ceramics body.

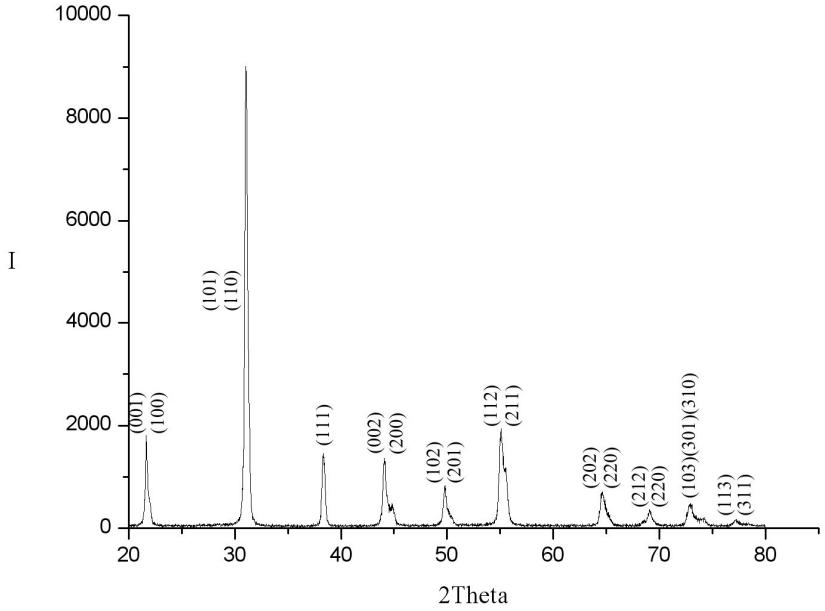

Fig. 3. The XRD pattern of the sintered ceramics body.

In large (diameter/thickness) ratio piezoelectric ceramic disk, the vibration modes are classified into five groups [Ikegami et al., 1974]. They are radial (R) mode, edge (E) mode, thickness shear (TS) mode, thickness extensional (TE) mode and high-frequency radial (A) mode. The resonant frequency of radial (R) mode and high-frequency radial (A) mode are strongly dependent on the diameter of the piezoelectric ceramic disk. And the resonant frequency of edge (E) mode, thickness shear (TS) mode and thickness extensional (TE) mode are strongly dependent on the thickness of the piezoelectric ceramic disk. With the increasing of frequency, the radial (R) mode appears at first, and then are edge (E) mode, thickness shear (TS) mode and thickness extensional (TE) mode, the high-frequency radial (A) mode exist at most higher frequency.

The resonant spectrum ranging from 100 kHz to 1500 kHz of piezoelectric ceramics disks with fully electrode size is show in Fig.4. From the results of Fig.4, it found that when the electrode is fully coating, there are one fundamental radial vibration mode (R), seven radial overtone modes (R1 to R7) and two edge modes (E) were existed in the frequency ranging from 100 kHz to 1500 kHz. The mode shapes of the fundamental radial vibration mode and its overtone are shown in Fig.5. It can see that the wave number increases with the frequency. The mode shape of edge mode is shown in Fig.6, the mode shape of edge mode is similar to that of radial modes except that the axial displacement at the edge is large, whereas it approaches zero in the radial modes [Guo & Cawley, 1992].

In the radial vibration mode, besides the fundamental mode, there are some overtone modes with inharmonic frequency separation. The series resonant frequency for the n^{th} vibration mode of the piezoelectric ceramic thin disk in the radial vibration mode can be expressed as [Randeraat & Setterington, 1974]:

$$f_{(sn)} = \frac{\alpha_n}{2\pi R}\sqrt{\frac{1}{s_{11}^E \rho(1-\sigma^2)}} \tag{21}$$

where s^E_{11} is compliance and $\sigma = -s^E_{12}/s^E_{11}$ was Poisson's ratio for the piezoelectric ceramic used in this study.

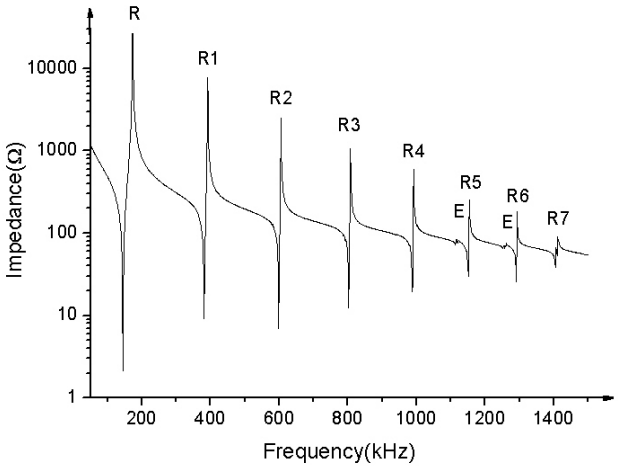

Fig. 4. The resonant spectrums of piezoelectric ceramics disk with fully electrode.

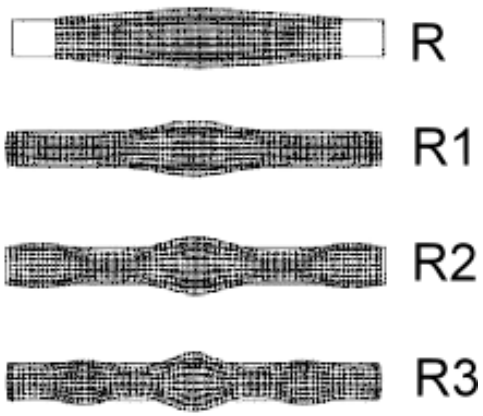

Fig. 5. The mode shapes of the radial vibration modes.

Fig. 6. The mode shape of edge mode.

For the piezoelectric ceramic disk in radial vibration mode, the ratio between the fundamental series resonant frequency and the overtones series resonant frequencies are not integers, but with a values equal to α_n/α_1, in which α_1 is the coefficient corresponding to the fundamental mode and α_n is the coefficient corresponding to the n^{th} order overtone vibration mode as shown in Eq.(21). The relation between overtones mode orders and the coefficient α_n and coefficient ratio α_n/α_1 were shown in Fig.7, and can be fit with second order polynomial:

$$\alpha_n = -1.83482 + 3.96149x - 0.15542x^2 \tag{22}$$

$$\alpha_n/\alpha_1 = -0.89661 + 1.94149x - 0.07613x^2 \tag{23}$$

where x is the mode orders.

The coefficient α_n and coefficient ratio α_n/α_1 increased with the increasing of overtones mode order, but the slope of coefficient ratio α_n/α_1 curve was less than that of coefficient α_n curve. It means that the separation between vibrations modes would decreased with the increasing of overtone mode order.

The planar effective electromechanical coupling factor k_p is decreased with the increasing in overtone mode order also, as shown in Fig.8, it also can be fit with second order polynomial:

$$k_p = 0.70566 - 0.23079x + 0.01959x^2 \tag{24}$$

The decrease of planar effective electromechanical coupling factor k_p with the increase in overtone mode order can be explained by the vibration mode shape. In radial vibration mode, when the electrical voltage is applied in the thickness direction, the disk contracts in the radial direction, and expands in the thickness direction, due to Poisson's ratio effects. The vibration mode shapes for the fundamental radial vibration mode, and the six radial overtone modes are predicted by the finite element method and shown in Fig. 5. From the results of Fig.5, it found that the contraction of the disk in the radial direction is the largest for fundamental radial vibration mode, and it decreases with the increasing of overtone mode order. The meaning of such phenomenon is that the electrical energy transfer to mechanical energy is decreased with the increasing of overtone mode order. As a result, the planar effective electromechanical coupling factor k_p is decreased with the increasing of overtone mode order.

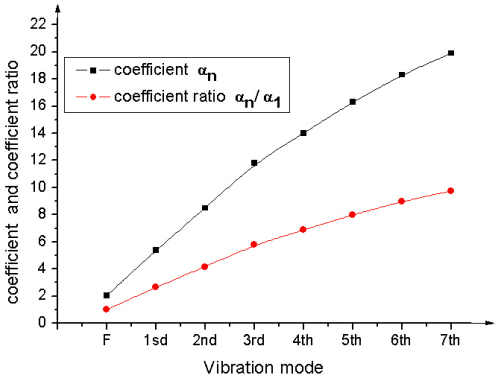

Fig. 7. The variation of coefficient α_n and coefficient ratio α_n/α_1 with mode orders.

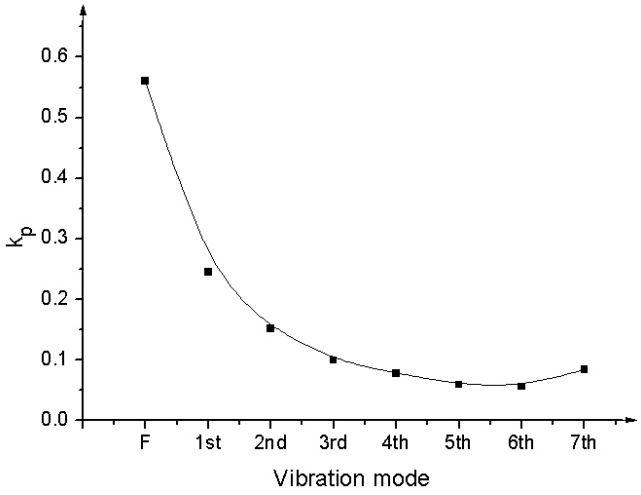

Fig. 8. The variation of electromechanical coupling factor k_p with mode orders.

When the electrode is reduced, the resonant spectrum will shift to higher frequency range, as shown in Fig. 9. The minimum impedance corresponding to series resonant frequency increased with the decreasing of electrode size. The maximum impedance corresponding to parallel resonant frequency also increased with the decreasing of electrode size, but when the electrode size reduced to less than 50%, the maximum impedance is decreased with the decreasing of electrode size.

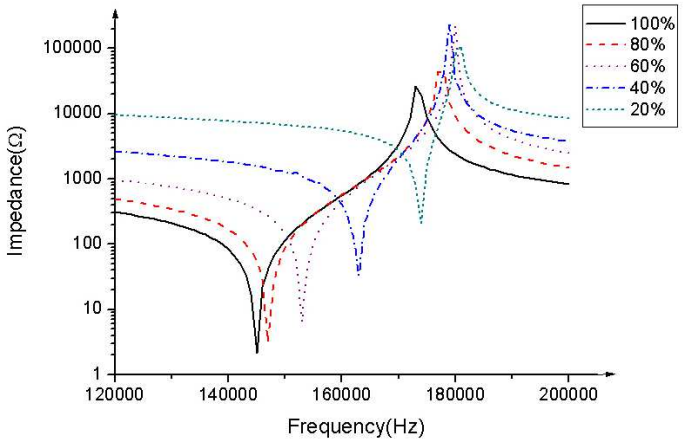

Fig. 9. Resonant spectrum of piezoelectric ceramic disk with different electrode size.

The series resonant and parallel resonant frequencies of fundamental radial vibration modes are increased with the decreasing of electrode size, but the planar effective electromechanical coupling factor is decreased with the decreasing of electrode size, as shown in Fig.10.

The relation between series resonant frequency (f_s) and planar effective electromechanical coupling factor (k_p) with electrode size (D_e) is second order polynomial and can be expressed as:

$$f_s=189-0.80857(D_e)+0.0357(D_e)^2 \quad (25)$$

$$k_p=0.0642+0.1136(D_e)-6.43929x10^{-5}(D_e)^2 \quad (26)$$

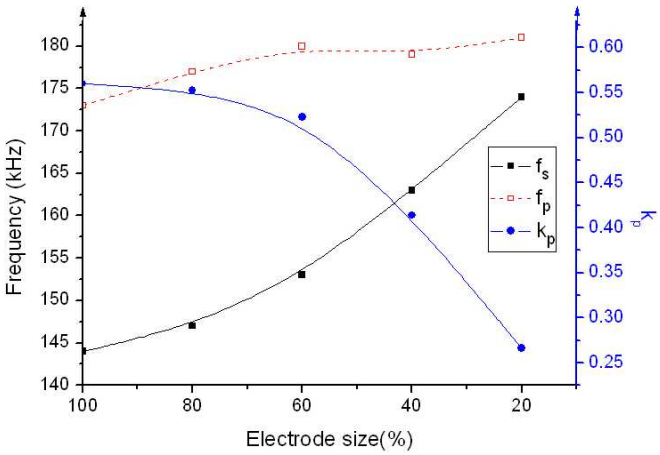

Fig. 10. The relation between electrode size and the electromechanical coupling factor k_p.

The frequency spectrums of different diameter-to-thickness ratio are shown in Fig.11 to Fig.14. From the results of these figures, it found that the numbers of radial vibration overtone mode are increased with the increasing of (D/t) ratio.

Besides the fundamental mode, there are eight radial vibration overtone modes are existed in the measured frequency range for (D/t) = 20.16. When the (D/t) decreased to 16.13, only six radial vibration overtone modes are existed in the measured frequency range. When the (D/t) ratio was larger than 15, only radial vibration mode is existed in the measured frequency range. When the (D/t) was less than 15, the numbers of radial vibration overtone mode reduced, and some other vibration modes will exist in the high frequency range. For (D/t) = 12.08 and 7.25, only five and three radial vibration overtone modes are existed in the measured frequency range, respectively. When the measured frequency higher than 600 kHz, some spurious vibration signals existed in the spectrum, these spurious vibration signals may be caused by other vibration mode; such as twist mode, bending mode or thickness mode. The relation between (overtone mode resonant frequency/fundamental resonant frequency) ratio and (diameter/thickness) ratio was shows in Fig.15. The (overtone mode resonant frequency/fundamental resonant frequency) ratio are increased with the increasing of (diameter/thickness) ratio.

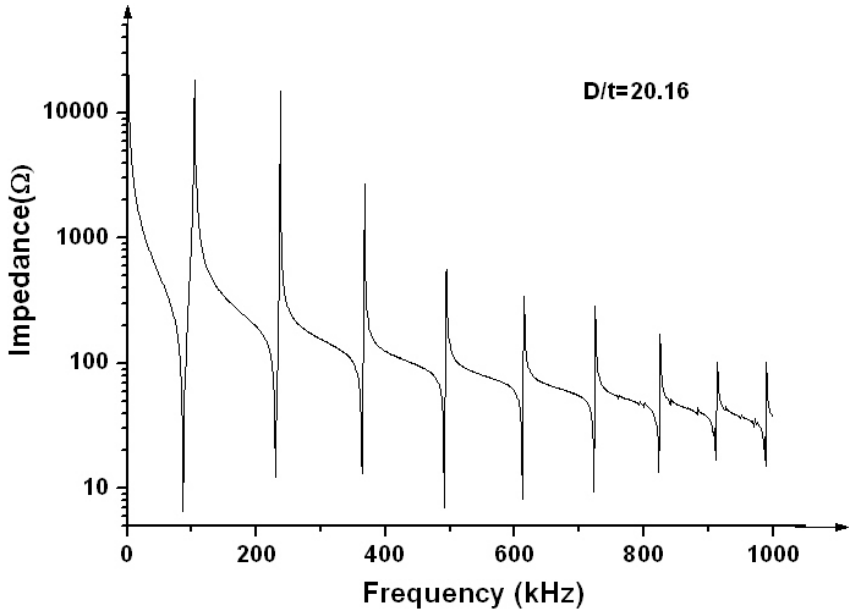

Fig. 11. The frequency spectrums of piezoelectric ceramic disk with D/t=20.16.

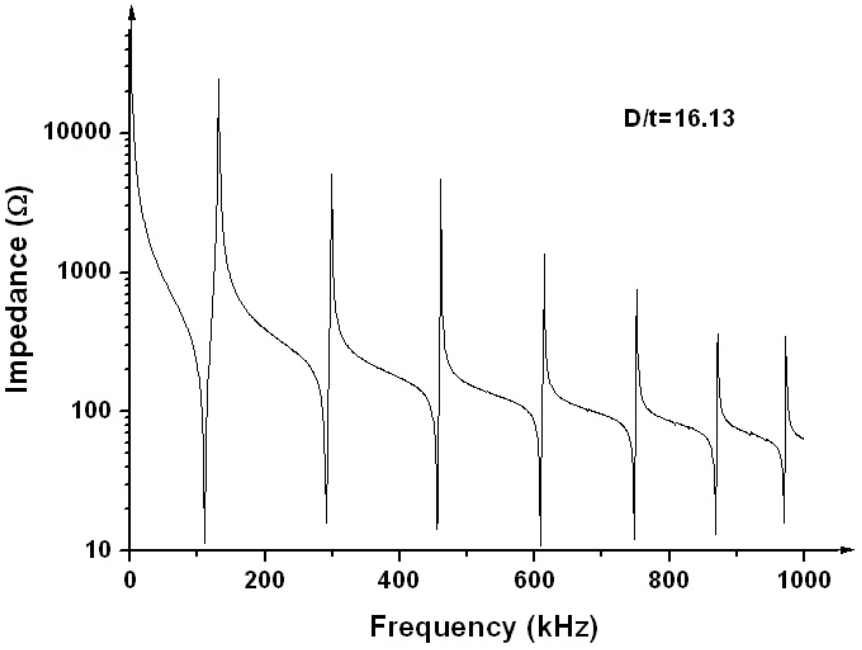

Fig. 12. The frequency spectrums of piezoelectric ceramic disk with D/t=16.13.

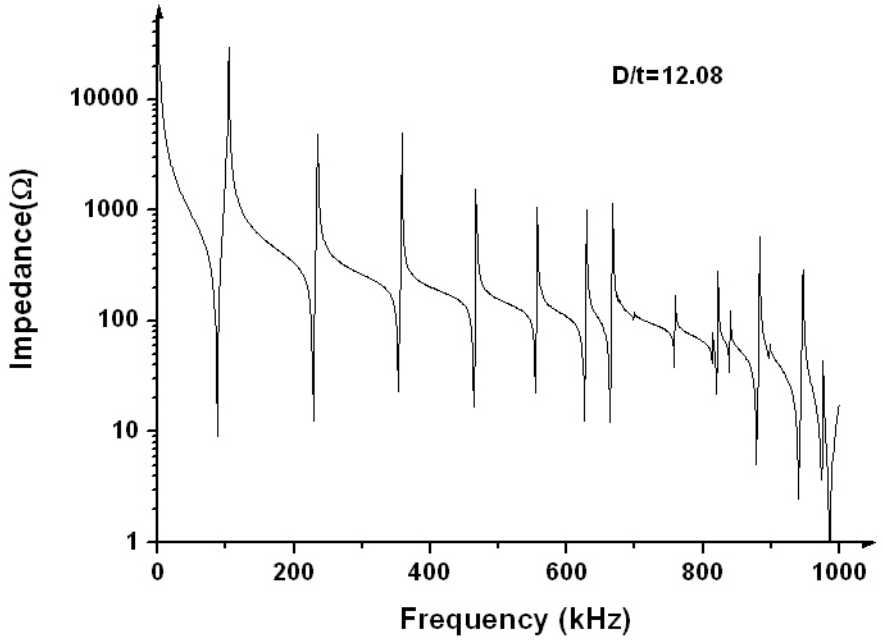

Fig. 13. The frequency spectrums of piezoelectric ceramic disk with D/t=12.08.

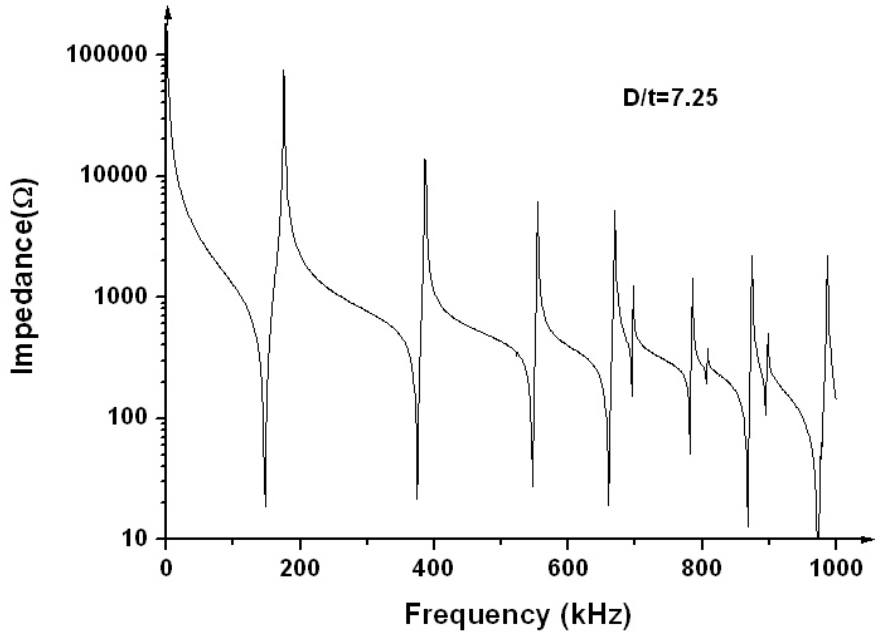

Fig. 14. The frequency spectrums of piezoelectric ceramic disk with D/t=7.25.

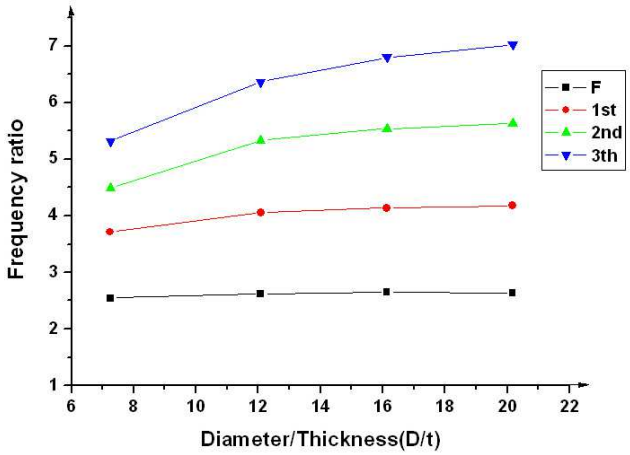

Fig. 15. Relation between (overtone mode resonant frequency/fundamental resonant frequency) ratio and (diameter/thickness) ratio.

5. Conclusion

For piezoelectric ceramic thin disk with larger (diameter/thick) ratio, in the lower frequency range, the major vibration mode is radial vibration mode. In the radial vibration mode, besides the fundamental mode, there are some overtone modes with inharmonic frequency separation. The planar effective electromechanical coupling factor k_p is decreased with the increasing in overtone mode order. The relation between planar effective electromechanical coupling factor and overtone mode order can be fit with second order polynomial.

When the electrode is reduced, the resonant spectrum will shift to higher frequency range, and the planar effective electromechanical coupling factor is decreased with the decreasing of electrode size.

The numbers of overtones mode are increased with the increasing of (D/t) ratio. The (overtone mode resonant frequency/fundamental resonant frequency) ratio are increased with the increasing of (diameter/thickness) ratio.

6. References

GuO, N. & Cawley, P. (1992). Measurement and Prediction of the Frequency Spectrum of Piezoelectric Disks by Modal Analysis, *The Journal of The Acoustical Society of America*, Vol.92, No.6, pp.3379-3388, ISSN 0001-4966

Guo, N.; Cawley, P. & Hitchings, D. (1992). The Finite Element Analysis of the Vibration Characteristics of Piezoelectric Discs, *Journal of Sound and Vibration*, Vol..159, No.1, pp.115– 38, ISSN 0022-460X

Haertling, G.H. (1999). Ferroelectric Ceramics: History and Technology, *Journal of the American Ceramic Society*, Vol.82, Issue.4, pp.797–818, ISSN 1551-2916

Huang, C.H. (2005). Theoretical and Experimental Vibration Analysis for a Piezoceramic Disk Partially Covered with Electrodes, *The Journal of The Acoustical Society of America,* Vol. 118, No.2, pp.751-761, ISSN 0001-4966

Huang, C.H.; Lin, Y.C. &Ma, C.C. (2004). Theoretical Analysis and Experimental Measurement for Resonant Vibration of Piezoceramic Circular Plates, *IEEE Transactions on Ultrasonics Ferroelectrics and Frequency Control*, Vol. 51, No. 1, pp.12–24, ISSN 0885-3010

IEEE Standard on Piezoelectricity, 176-1987, ANSI-IEEE Std. 176, 1987.

Ikegami, S.; Ueda, I. & Kobayashi, S. (1974). Frequency Spectrum of Resonant Vibration in Disk Plates of $PbTiO_3$ Piezoelectric Ceramics, *The Journal of The Acoustical Society of America,* Vol.55, No.2, pp.339-344, ISSN 0001-4966

Ivina, N. F. (1990). Numerical Analysis of the Normal Modes of Circular Piezoelectric Plates of Finite Dimensions, *Soviet Physics – Acoustics,* Vol.35, No.4, pp.385–388, ISSN 0038-562X

Ivina, N. F. (2001). Analysis of the Natural Vibrations of Circular Piezoceramic Plates with Partial Electrodes, *Acoustical Physics*, Vol.47, No.6, pp.714–720, ISSN 1652-6865

Jaffe, B.; Cook, W.R. & Jaffe, H. (1971). *Piezoelectric Ceramics*, Academic Press, ISBN 0-12-379550-8, New York, U.S.A.

Kunkel, H. A.; Locke, S. & Pikeroen, B. (1990). Finite-Element Analysis of Vibrational Modes in Piezoelectric Ceramics Disks, *IEEE Transactions on Ultrasonics Ferroelectrics and Frequency Control*, Vol. 37, No. 4, pp.316–328, ISSN 0885-3010

Masaki, M.; Hashimoto, H.; Masahiko, W. & Suzuki, I. (2008). Measurements of Complex Materials Constants of Piezoelectric Ceramics: Radial Vibrational Mode of a Ceramic Disk, *Journal of the European Ceramic Society*, Vol.28, Issue.1, pp.133–138, ISSN 0955-2219

Moulson, A.J. & Herbert, J.M. (1997). *Electroceramics: Materials, Properties, Applications*, Chapman and Hall, ISBN 0-412-29490-7, London, England

Newnham, R.E. & Ruschau, G.R. (1991). Smart Electroceramics, *Journal of the American Ceramic Society*, Vol.74, Issue.3, pp. 463–480, ISSN 1551-2916

Randeraat, J.V. & Setterington, R.E. (1974). *Piezoelectric Ceramics*, Mullard House, ISBN 0-901232-75-0, London, England

Rogacheva, N.N. (1994). *The Theory of Piezoelectric Shells and Plates*, ISBN-10:084934459X, CRC Press, Boca Raton, Florida, USA

Shaw, E.A.G. (1956). On the Resonant Vibrations of Thick Barium Titanate Disks, *The Journal of the Acoustical Society of America,* Vol.28, No.1, pp.38-50, ISSN 0001-4966

Schmidt, G. H. (1972). Extensional Vibrations of Piezoelectric Plates, *Journal of Engineering Mathematics*, Vol. 6, No. 2, pp.133–142, ISSN 0022-0833

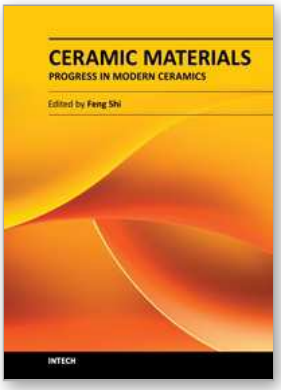

Ceramic Materials - Progress in Modern Ceramics

Edited by Prof. Feng Shi

ISBN 978-953-51-0476-6
Hard cover, 228 pages
Publisher InTech
Published online 05, April, 2012
Published in print edition April, 2012

This text covers ceramic materials from the fundamentals to industrial applications. This includes their impact on the modern technologies, including nano-ceramic, ceramic matrix composites, nanostructured ceramic membranes, porous ceramics, and the sintering theory model of modern ceramics.

InTech Europe
University Campus STeP Ri
Slavka Krautzeka 83/A
51000 Rijeka, Croatia
Phone: +385 (51) 770 447
Fax: +385 (51) 686 166
www.intechopen.com

InTech China
Unit 405, Office Block, Hotel Equatorial Shanghai
No.65, Yan An Road (West), Shanghai, 200040, China
中国上海市延安西路65号上海国际贵都大饭店办公楼405单元
Phone: +86-21-62489820
Fax: +86-21-62489821